Supplementary Information

A self-sufficient pressure pump using latex balloons for microfluidic applications

Peter Thurgood [1,†], Jiu Yang Zhu [1], Ngan Nguyen [1], Saeid Nahavandi [2], Aaron R. Jex [3,4], Elena Pirogova [1] , Sara Baratchi [5], Khashayar Khoshmanesh [1,†]

[1] School of Engineering, RMIT University, Melbourne, Australia

[2] Institute for Intelligent Systems Research and Innovation, Deakin University, Waurn Ponds, Australia

[3] Population Health and Immunity Division, The Walter and Eliza Hall Institute of Medical Research, Parkville, Australia

[4] Faculty of Veterinary and Agricultural Sciences, The University of Melbourne, Parkville, Australia

[5] School of Health & Biomedical Sciences, RMIT University, Bundoora, Australia

† Corresponding authors:

Peter Thurgood: pthurgood@gmail.com

Khashayar Khoshmanesh: Khashayar.khoshmanesh@rmit.edu.au

Supplementary Information S1: The process of assembling the balloon pump and coupling it to our microfluidic system.

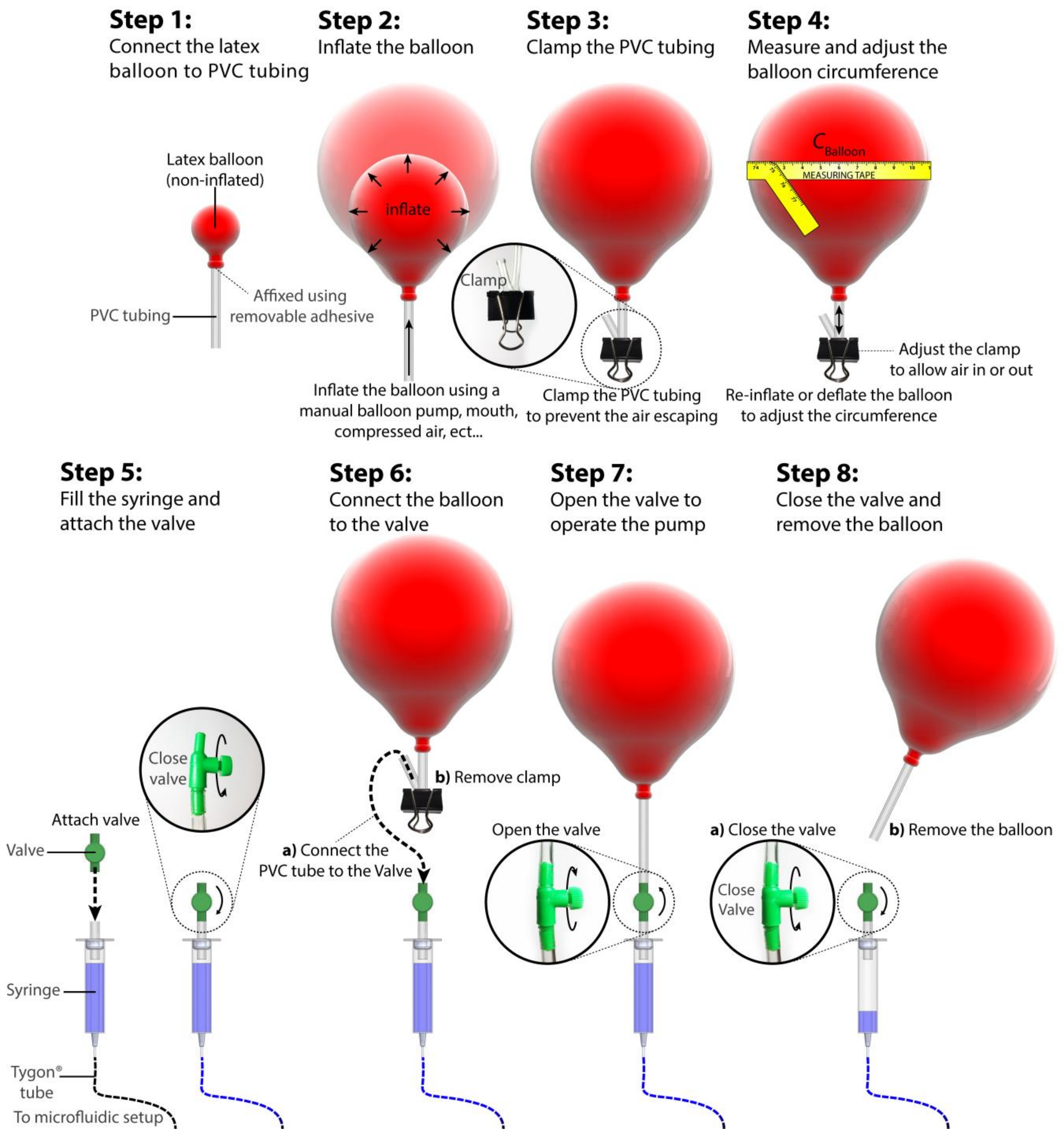

Figure S1: The step-by-step process of assembling the balloon pump and coupling it to our microfluidic system.

Supplementary Information S2: Photograph of experimental setup

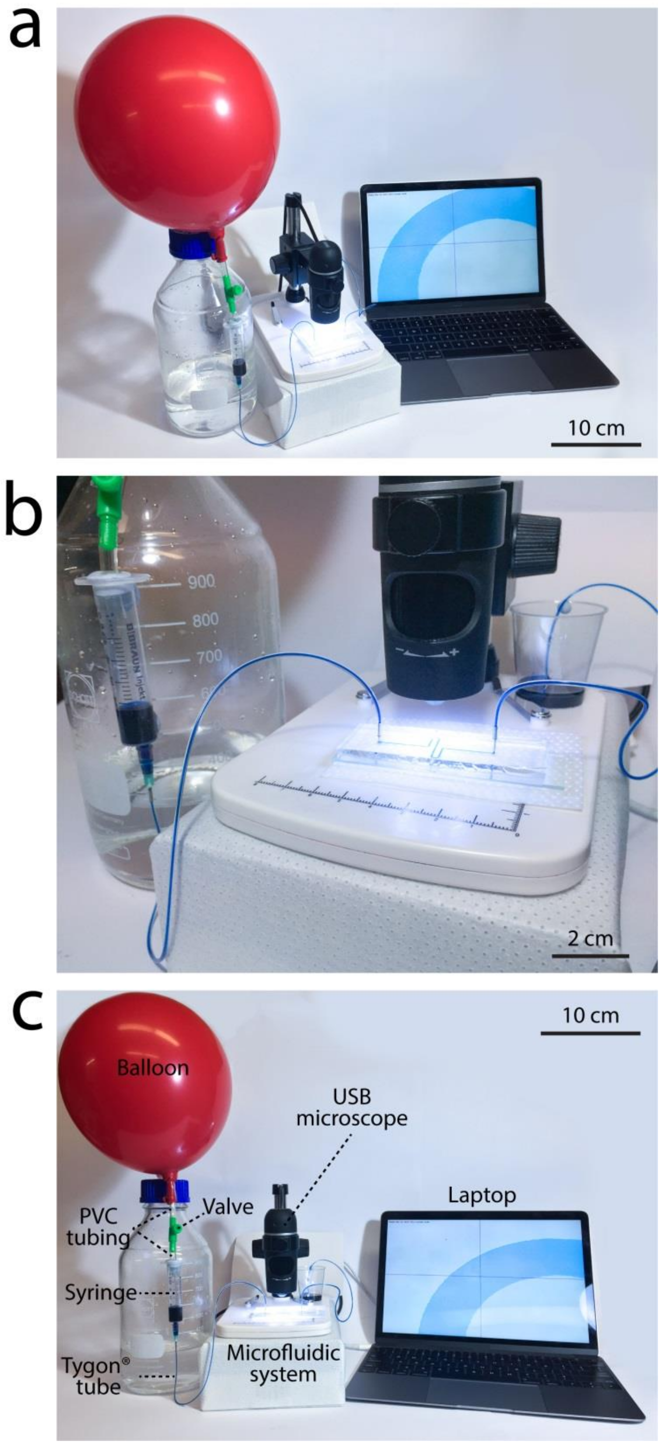

Figure S2: Photographs of the microfluidic system operated by a latex balloon.

Supplementary Information 3: Measurement of the inflation pressure of the balloon using a custom U-tube manometer

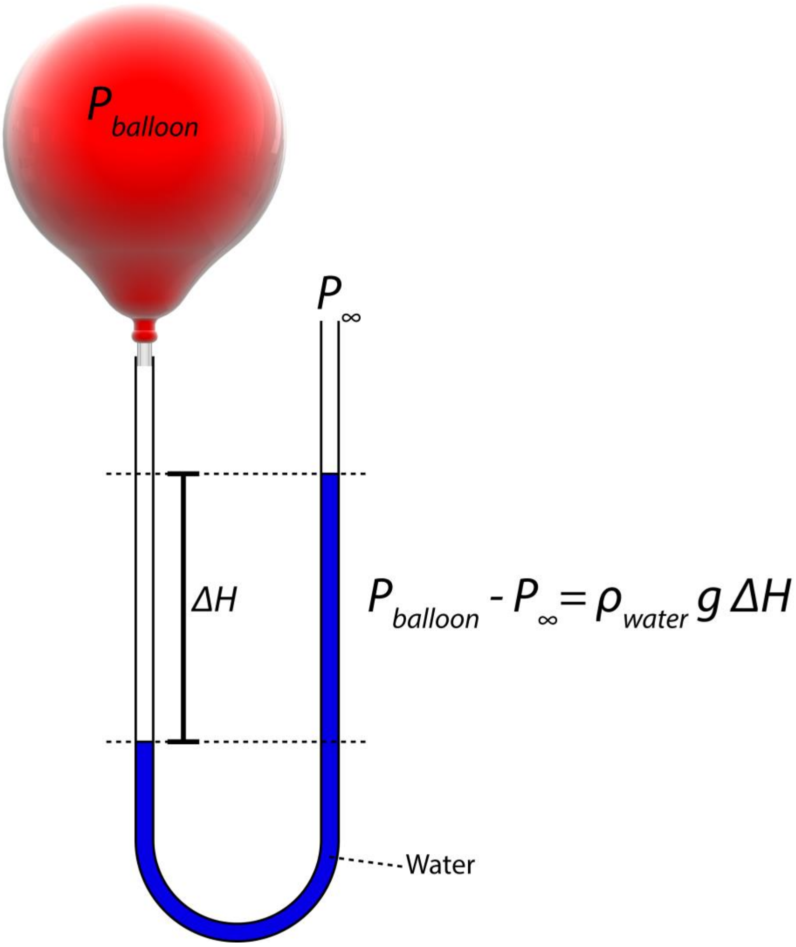

Figure S3: Custom U-tube manometer using PVC tubing (ID = 4 mm, OD = 6 mm) coupled to a helium quality latex balloon used to measure the inflation pressure of the balloon.

Supplementary Information 4: Schematics of the microfluidic channels

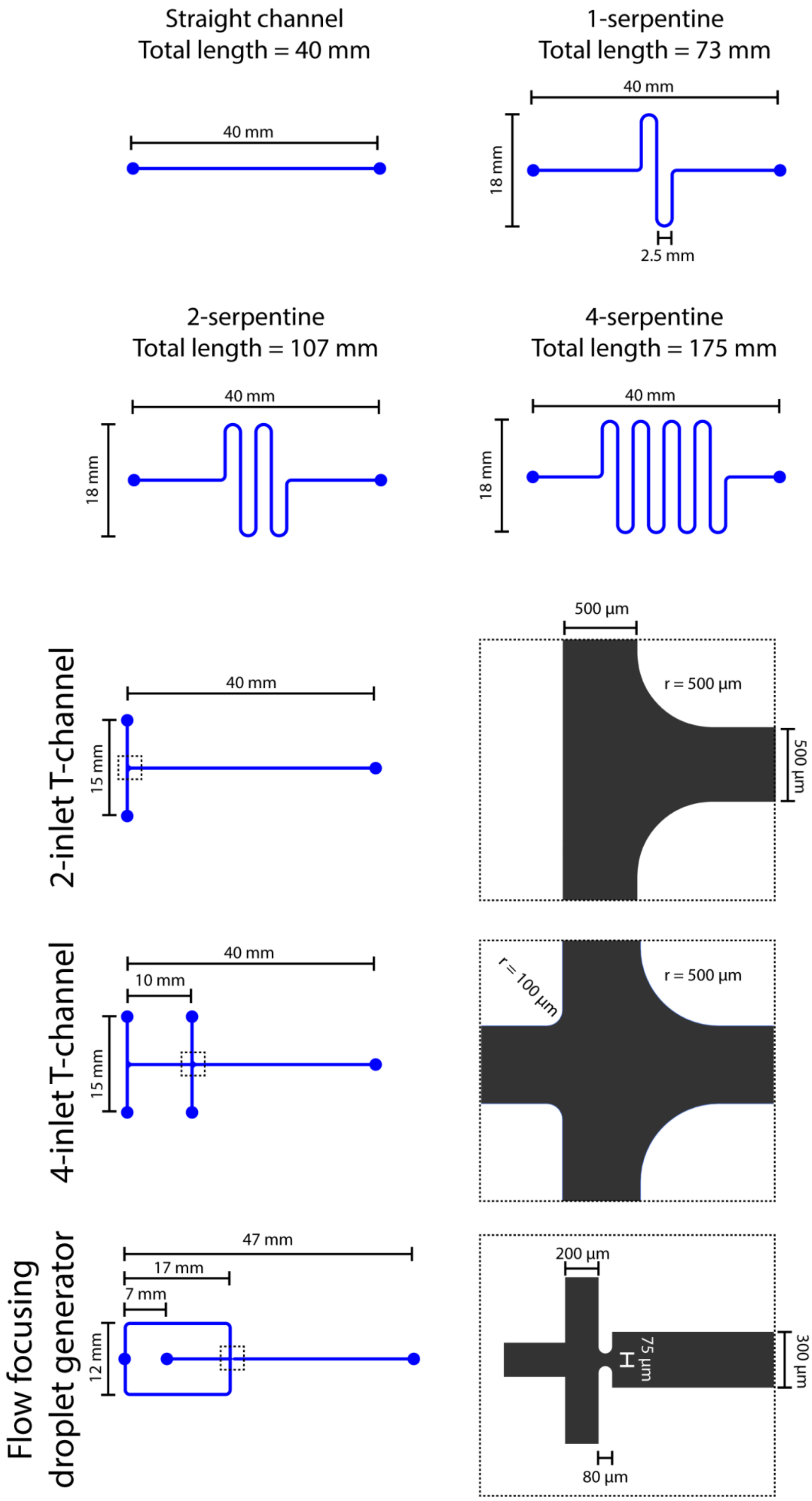

Figure S4: Details of straight, serpentine and multi-inlet microfluidic channels.

Supplementary Information 5: Details of curves fitted to raw data points shown in **Figure 2**

Table S1: Details of curve fitting models used for generation of smooth lines in **Figure 2**

Parameter	Figure	N	Fitted curve	R^2
Channel length	**2a**	6	$Q = 1877.7\, L_{\text{channel}}{}^{-0.903}$	0.9994
Liquid viscosity	**2b**	6	$Q = 66.96 \left(\frac{\mu}{\mu_{@23℃}}\right)^{-1.004}$	0.9997
Temperature	**2c**	3	$Q = 65.12 + 0.0484\exp(0.145\, T)$	0.9998
	2c-inset	3	$\frac{P_{\text{balloon}} - P_\infty}{P_{\text{balloon}} - P_\infty\rvert_{@23℃}} = 0.789 + 2.833\exp(-0.112\, T)$	0.99
	2c-inset	3	$\frac{\mu}{\mu_{@23℃}} = 0.327 + 1.491\exp(-0.0346\, T)$	0.99
Inflation numbers	**2d**	3	$Q_{C=75\,cm} = 66.56 + 190\exp(-2\, n_{inflation})$	0.998
	2d	3	$Q_{C=65\,cm} = 47.28 + 63.8\exp(-1.69\, n_{inflation})$	0.99
	2d	3	$Q_{C=55\,cm} = 38.33 + 36\exp(-1.54\, n_{inflation})$	0.997
Outlet height	**2e**	6	$Q = 67.2 - 3\,\text{H}_{outlet}$	0.98
Balloon circumference	**2g**	6	Smooth lines interpolated in Excel	NA

Legend:

N: Number of experimental repeats

Q: Flow rate (μL/min)

L_{channel}: Microfluidic channel length (mm)

$\frac{\mu}{\mu_{@23℃}}$: Viscosity ratio

$\frac{P_{\text{balloon}} - P_\infty}{P_{\text{balloon}} - P_\infty\rvert_{@23℃}}$: Balloon inflation pressure ratio

T: Temperature (°C)

C: Balloon circumference (cm)

$n_{inflation}$: Number of successive balloon inflations

H_{outlet}: Outlet tube height (mm)

Supplementary Information 6: Zoomed-in raw data points collected by digital scale over 30, 5 and 1 minutes for the 75 cm balloon

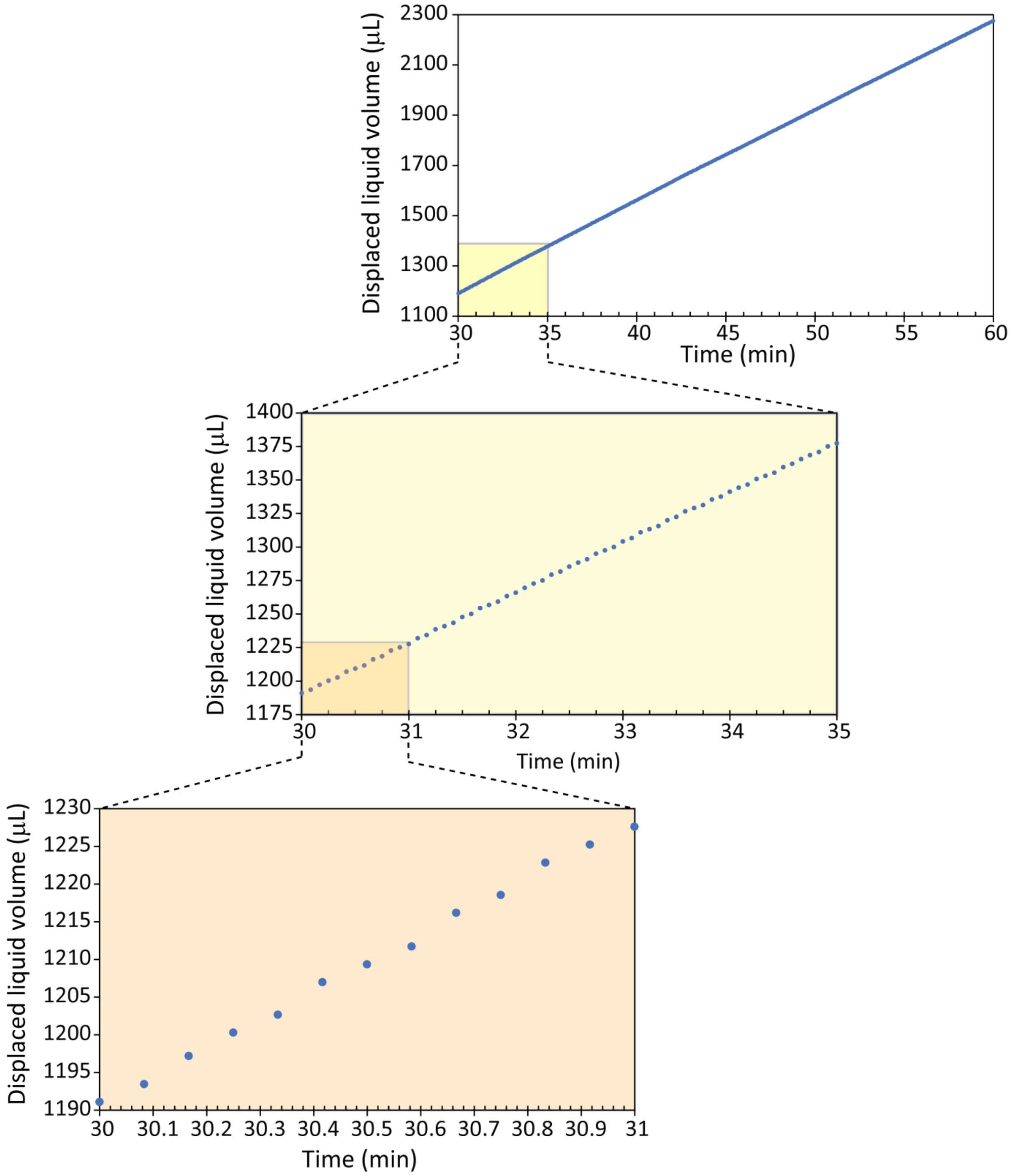

Figure S5: Zoomed-in raw data points collected by digital scale over 30, 5 and 1 minutes for the 75 cm balloon.

Supplementary Information 7: Reduction of balloon circumference over a 12-hour period for various balloons

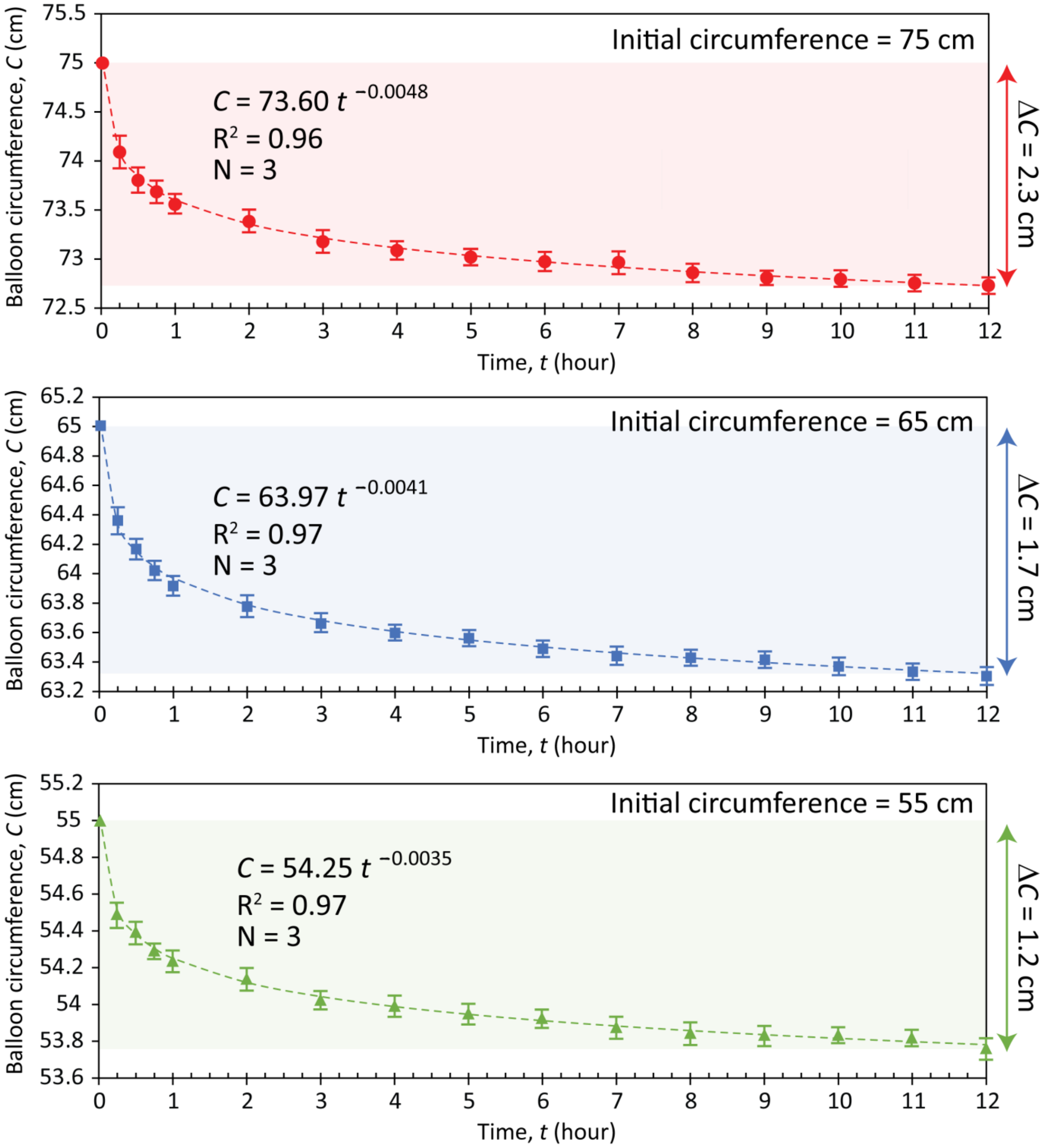

Figure S6: Reduction of balloon circumference over a 12-hour period for the balloons with initial circumferences of 75, 65 and 55 cm. Error bars represent average ± STD values obtained from three sets of independent experiments.

Supplementary Information 8: Close-up of flow rates over the first two hours of balloon pump operation

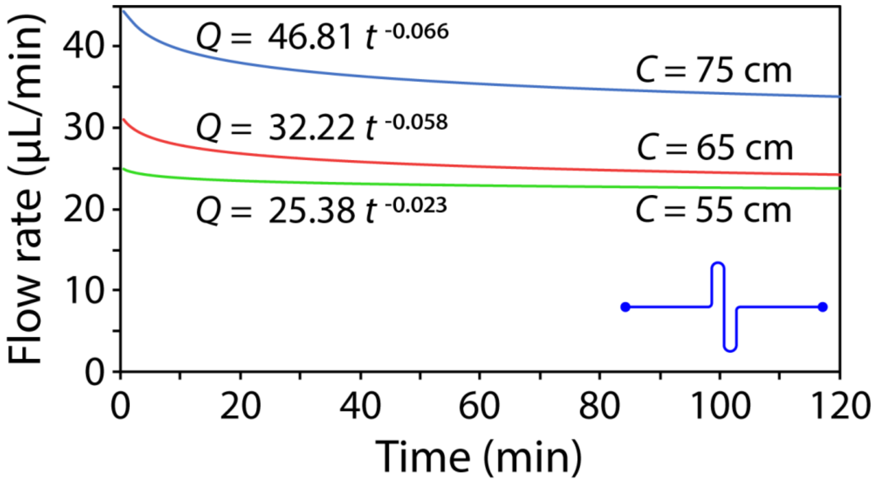

Figure S7: The *flow rate* vs. *time* curves over the first two hours of balloon operation. The *flow rate* vs. *time* equations were obtained by differentiating the *displaced liquid volume* vs. *time* equations obtained in **Figure 2f**.

Supplementary Information 9: The effect of balloon shell thickness on its pumping performance.

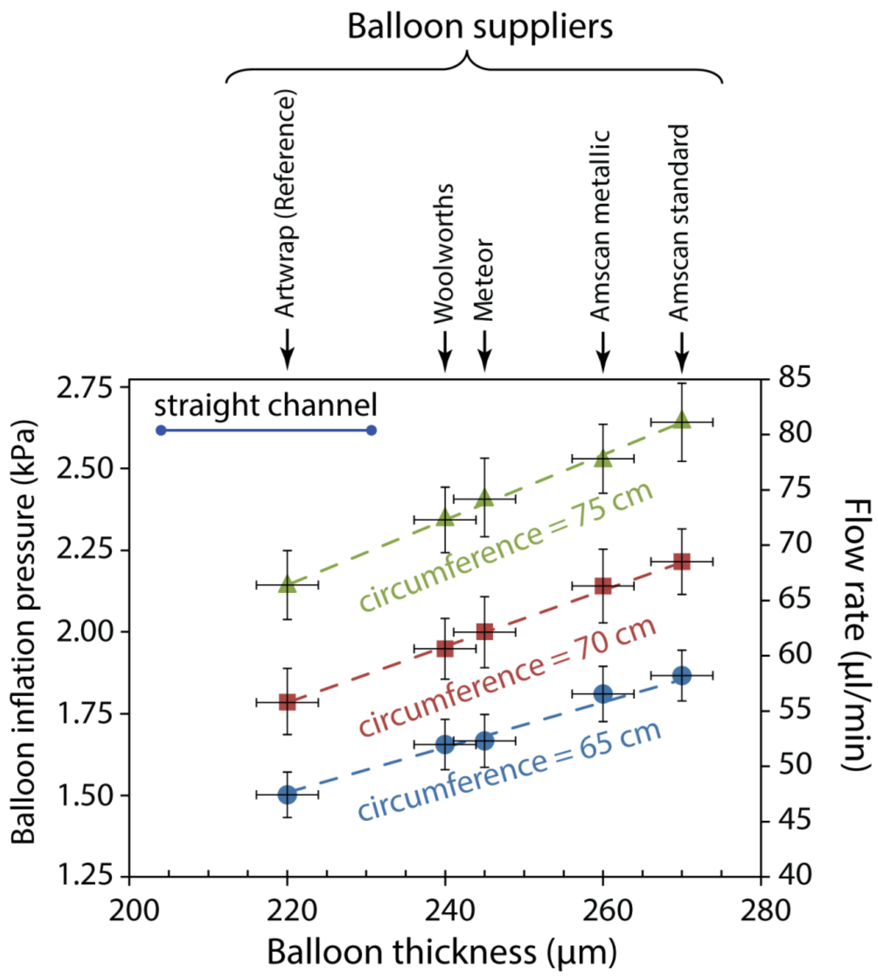

Figure S8: Variations of balloon inflation pressure and induced flow rate though the straight reference channel against balloon shell thickness for five helium quality balloons available in Australian supermarkets. Error bars represent average ± STD values obtained from at least six sets of independent experiments.

Supplementary Information 10: Pressure contours along the T-channel operated by two balloon pumps obtained by numerical simulations

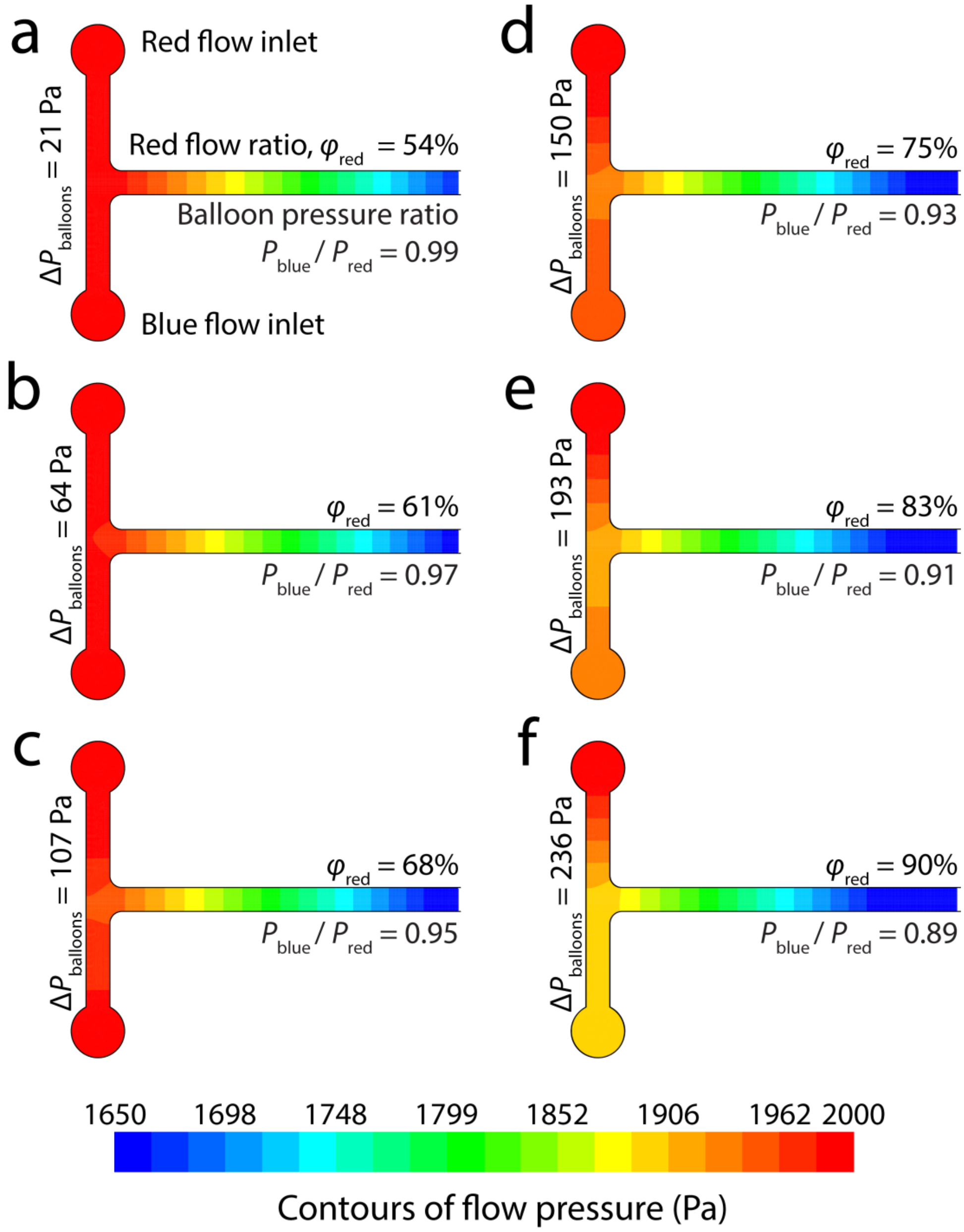

Figure S9: Pressure contours across the T-channel under various pressure ratios of the balloons (P_{blue}/P_{red}) obtained by numerical simulations. The values of pressure differences between the balloons ($\Delta P_{balloons} = P_{red} - P_{blue}$) is also given.

Supplementary Information 11: Pressure contours

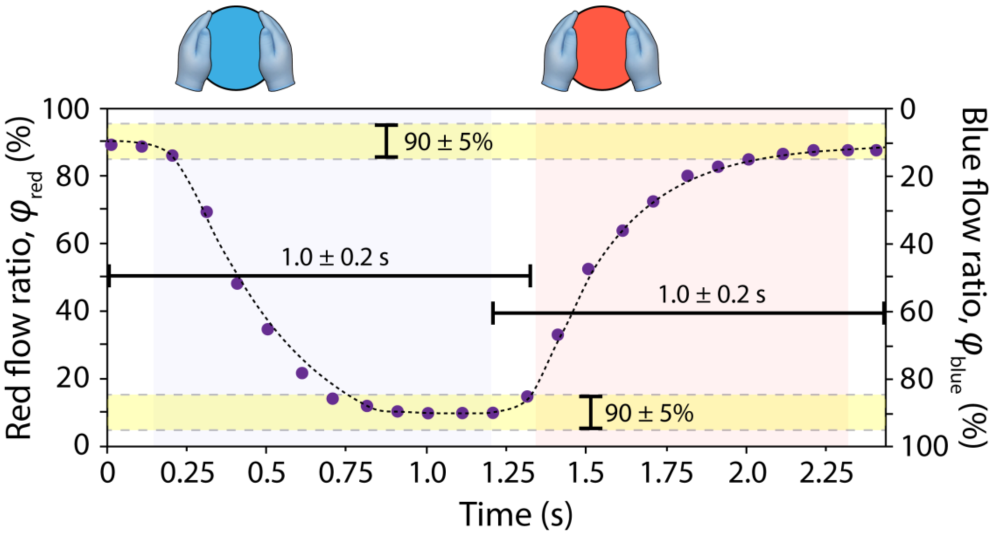

Figure S10: Error bars represent average ± STD values based on three successive cycles.

Supplementary Information 12: Numerical simulations corresponding to the passive mixing of four neighbouring liquids in a four-inlet microfluidic channel operated by four balloon pumps

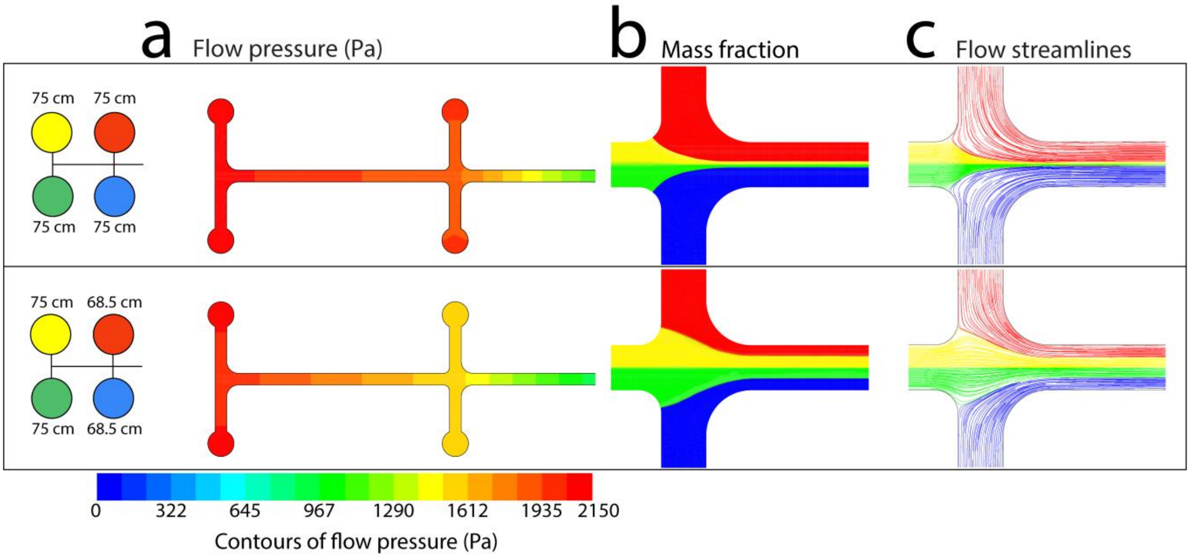

Figure S11: Numerical simulations corresponding to the passive mixing of four neighbouring liquids in a four-inlet microfluidic channel operated by four balloon pumps: **(a)** Contours of pressure with the insets showing the circumference of the balloons. **(b)** Contours of mass fraction at the junction of the channel. **(c)** Flow streamlines coloured according to the mass fraction of liquids.

Supplementary Information 13: Droplet diameter profiles over five successive dynamic squeezing cycles

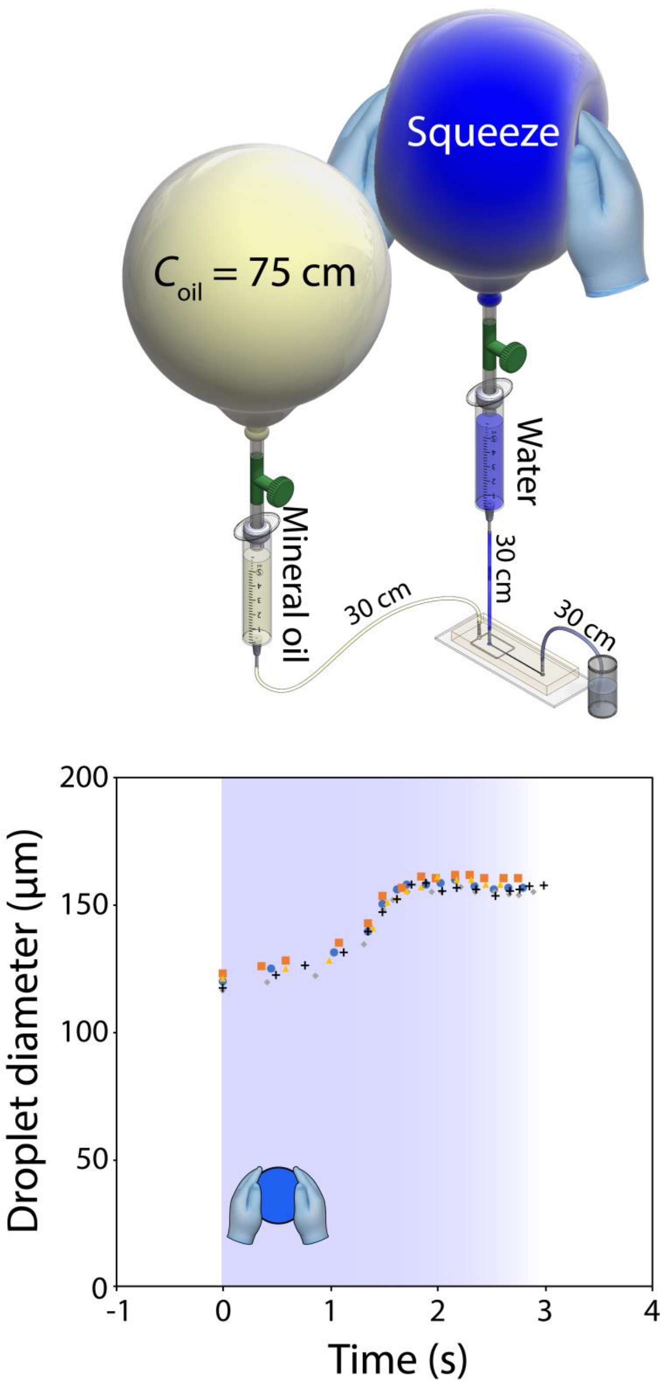

Figure S12: Variations of droplet diameter over five successive cycles stacked within one cycle.